

Received: 2019.05.19  
Accepted: 2019.07.31  
Published: 2019.08.14

# Irisin Enhances Doxorubicin-Induced Cell Apoptosis in Pancreatic Cancer by Inhibiting the PI3K/AKT/NF- $\kappa$ B Pathway

Authors' Contribution:  
Study Design A  
Data Collection B  
Statistical Analysis C  
Data Interpretation D  
Manuscript Preparation E  
Literature Search F  
Funds Collection G

ABCDEF 1,2 **Jiayu Liu**  
ACDF 1,2 **Yibing Huang**  
ACEG 3 **Yu Liu**  
ACEG 1,2 **Yuxin Chen**

1 Key Laboratory for Molecular Enzymology and Engineering of The Ministry of Education, Jilin University, Changchun, Jilin, P.R. China  
2 School of Life Sciences, Jilin University, Changchun, Jilin, P.R. China  
3 Department of Endocrinology, Sir Run Run Hospital, Nanjing Medical University, Nanjing, Jiangsu, P.R. China

**Corresponding Authors:** Yu Liu, e-mail: drliuyu@njmu.edu.cn, Yuxin Chen, e-mail: chen\_yuxin@jlu.edu.cn

**Source of support:** This work was supported by the National Key Research and Development Program of China (2016YFC1305000, 2016YFC1305005 to YL), the National Natural Science Foundation of China (81770778, 81570704 to YL), and the Natural Science Foundation of Jilin Province of China (20180101250 JC to YBH)

**Background:** Irisin, a myokine released from skeletal muscle following exercise, has been shown to affect the proliferation of some cancer cells and chemosensitivity of anticancer drugs like doxorubicin (DOX). However, the effects of irisin on chemosensitivity in pancreatic cancer (PC) cells have not been studied.





**Material/Methods:** In this study, the effects of irisin co-treatment with DOX or gemcitabine (GEM) on MIA PaCa-2, BxPC-3 PC cells, and H9c2 cardiomyocytes were investigated. MTT (3-(4,5-dimethylthiazol-2-yl)-2,5-diphenyltetrazolium bromide) assay, flow cytometry, and TUNEL (TdT-mediated dUTP nick-end labeling) assays were conducted to evaluate cytotoxicity induced by DOX or GEM. Fluorescence microscopy and flow cytometry experiments were performed to assess the intracellular accumulation of DOX. Cellular levels of apoptosis-related protein expression and protein phosphorylation were determined by Western blot analyses.

**Results:** The results showed that irisin can increase the chemosensitivity of PC cells to DOX or GEM. The analyses of apoptosis indicated that irisin enhances DOX-induced cellular apoptosis by increasing the expression of cleaved PARP (poly ADP-ribose polymerase) and cleaved caspase-3, and reducing the expression of B cell lymphoma/leukemia-2 (BCL-2) and B cell lymphoma-extra large (BCL-xL) in PC cells but not in H9c2 cells. Irisin attenuated serine/threonine kinase AKT (protein kinase B/PKB) phosphorylation and inhibited the activation of nuclear factor  $\kappa$ B (NF- $\kappa$ B) signaling in PC cells.

**Conclusions:** Irisin can potentiate the cytotoxicity of doxorubicin in PC cells without increasing cardiotoxicity, possibly through inactivating the PI3K/AKT/NF- $\kappa$ B signaling pathway.

**MeSH Keywords:** **Apoptosis Inducing Factor • Doxorubicin • Pancreatic Neoplasms**

**Full-text PDF:** <https://www.medscimonit.com/abstract/index/idArt/917625>

 3512   7  47



## Background

Pancreatic cancer (PC) is a high-mortality disease. At present, early diagnosis of PC still remains difficult [1]. However, current therapeutic strategies are not very effective in increasing patient survival [2]. Currently, 5-year relative survival is still below 8% [3]. Thus, new treatment strategies for PC are the focus of current research.

Gemcitabine (GEM) is a cycle-specific, anti-metabolic, anti-tumor drug that mainly acts on tumor cells in the DNA synthesis phase (S phase), GEM alone, or in combination with other agents, and remains the standard of treatment method for PC. However, many PC cells are resistant to GEM, which makes it very difficult to treat [4]. Doxorubicin (DOX) is an anthracycline antibiotic and a first-line anti-tumor drug for the treatment of a wide variety of cancers, but free DOX has adverse effects of irreversible cardiomyopathy and heart failure, which limit its clinical uses [5,6]. However, DOX treatment often results in the development of resistance in many cancer types. Chemoresistance of DOX is a complex process involving the regulation of many cellular biology processes through various mechanisms, including increased expression of p-glycoprotein efflux transporter protein [7, 8]. Many studies have suggested that inhibition of the PI3K/AKT and NF- $\kappa$ B pathways plays an important role in improving the effectiveness of DOX [9,10]. The PI3K/AKT pathway plays a crucial role in cell proliferation, survival, and drug resistance through regulating multiple downstream cascades in various cancers, including PC cells [11,12]. Once activated, AKT can phosphorylate multiple substrates and downstream effectors, such as the mammalian target of rapamycin (mTOR) family, caspases, cell cycle proteins, and NF- $\kappa$ B [9]. NF- $\kappa$ B also has a therapeutic effect in ameliorating chemoresistance [13,14]. NF- $\kappa$ B proteins in resting cells are retained in the cytoplasm in relation to inhibitory I $\kappa$ B proteins. When activated, I $\kappa$ B- $\alpha$  is phosphorylated by I $\kappa$ B kinase, leading to the ubiquitination and subsequent degradation of I $\kappa$ B- $\alpha$  by the proteasome with cooperative phosphorylation of p65 [15,16].

Irisin is a recently discovered myokine secreted from skeletal myocytes during exercise, which can induce the browning of white adipose tissues (WAT) [17]. Irisin has been reported to play an important role in obesity and type 2 diabetes mellitus (T2DM), cardiovascular disease (CVD), and other metabolic diseases [18–21]. Obesity and type 2 diabetes (T2DM) have been reported to be PC-related risk factors, and overweight people have an increased risk of developing PC and mortality [22]. Aydin et al. found higher expression of irisin in ductal adenocarcinoma compared with normal pancreas tissue [23]. Recent studies indicated that irisin has effects on a number of tumor types and it has been reported to enhance the sensitivity of cancer cells to DOX [24,25]. Irisin has been

shown to participate in the PI3K/AKT signaling pathway when regulating various functions, such as protecting against endothelial injury and inhibiting hepatic gluconeogenesis [26,27]. Irisin has been reported to have an inhibitory effect in breast cancer cells and to make DOX more effective in breast cancer cells through NF- $\kappa$ B cell signaling [24], while in lung cancer cells, irisin can inhibit activation of the PI3K/AKT pathway [25].

An adverse effect of DOX is its long-term use leading to acute cardiotoxicity [28,29]. It has been reported that DOX has a lower response rate in PC when used as a single agent because of its drug resistance [28,30]. Thus, there is an urgent need to develop more effective therapeutic agents, used alone or in combination with DOX, to render PC more sensitive to DOX.

In this study, we evaluated the effects of irisin alone and in combination with DOX or GEM on cell viabilities and apoptosis in PC cells. We also investigated the corresponding molecular mechanism by which irisin enhances DOX anti-tumor activity and the effects of irisin on DOX myocardial cytotoxicity.

## Material and Methods

### Reagents and antibodies

Irisin was expressed and purified as previously described [31]. DOX was purchased from Macklin (Shanghai, China). MTT from Sigma-Aldrich (St. Louis, MO, USA). Annexin V-FITC (fluorescein isothiocyanate) and propidium iodide (PI) Apoptosis Detection Kits were from BestBio (Shanghai, China). One-Step terminal deoxynucleotidyl transferase dUTP nick-end labeling (TUNEL) Apoptosis Assay Kits were from Meilune (Dalian, China). Hoechst 33258 was purchased from BestBio (Shanghai, China). Horseradish peroxidase (HRP)-conjugated secondary antibody, anti-PARP, and anti-cleaved caspase-3 antibodies were purchased from Cell Signaling Technology (Boston, MA, USA). Anti-total and anti-phosphorylated (Ser473) AKT, anti-BCL-2 and anti-BCL-xL, and anti- $\beta$ -actin rabbit antibodies were obtained from Affinity Biosciences (Cincinnati, OH, USA). Anti-total and anti-phosphorylated (Ser536) NF- $\kappa$ B p65 and anti-I $\kappa$ B- $\alpha$  antibodies were purchased from Wanleibio (Shenyang, China). FITC-conjugated secondary antibody was from BIOSS (Beijing, China).

### Cell culture

MIA PaCa-2, BxPC-3, and H9c2 cells were from ATCC (Manassas, VA, USA). Cells were cultured in DMEM medium (Gibco, NY, USA) with 10% fetal bovine serum (FBS) in an atmosphere of 5% CO<sub>2</sub> at 37°C.

### Cell viability assay

PC cells ( $1 \times 10^4$  cells/well) were cultured in 96-well plates in DMEM (10% FBS) for 12 h and then treated with DOX (0, 0.375, 0.75, 1.5, 3, 6, 12, and 24  $\mu\text{g}/\text{mL}$ ) combined with different concentrations of irisin (0, 5, 10, 50, and 100 nM) for 24 h. Cells were treated with GEM (0, 0.375, 0.75, 1.5, 3, 6, 12, 24, and 48  $\mu\text{g}/\text{mL}$ ) combined with different concentrations of irisin (0, 5, 10, 50, and 100 nM) for 48 h. H9c2 cells were treated with various concentrations of irisin for 24 h. Then, 20  $\mu\text{l}$  of MTT solution (5 mg/mL) was added to each well and incubated for an additional 4 h. Subsequently, the formazan crystals were dissolved in DMSO, and the OD at 570 nm was measured using an Infinite F200 Pro device (TECAN, Switzerland). GraphPad Prism 5.0 software was used to analyze the 50% inhibitive concentration ( $\text{IC}_{50}$ ).

### Flow cytometry

The Annexin V-FITC and propidium iodide (PI) Apoptosis Detection Kits were used to monitor the apoptosis levels using flow cytometry. Cells ( $1 \times 10^5$ ) were cultured in 12-well plates for 12 h, then exposed to irisin alone, GEM alone, or GEM in combination with irisin for 48 h. Cells for analysis were washed with phosphate-buffered saline (PBS), suspended in 400  $\mu\text{l}$  binding buffer, and stained with 5  $\mu\text{l}$  Annexin V-FITC and 5  $\mu\text{l}$  PI for 15 min in the dark. Cells were analyzed using flow cytometry (CytoFLEX, Beckman Coulter, IN, USA).

Cells were exposed to irisin alone, DOX alone, or DOX in combination with irisin for 24 h. After incubation, cells were exposed to irisin alone, DOX alone, or DOX in combination with irisin for 24 h. After incubation, cells were collected for measurement of DOX fluorescence using flow cytometry (CytoFLEX, Beckman Coulter, IN, USA).

### TUNEL assay

PC cells ( $1 \times 10^5$  cells/well) were cultured in 12-well plates in DMEM (10% FBS) for 12 h. Cells were then exposed to irisin alone, DOX alone, or DOX in combination with irisin for 24 h. Cells were fixed with 4% paraformaldehyde/PBS, washed with PBS, and then permeabilized with 0.1% Triton X-100 for 2 min on ice followed by TUNEL for 1 h at 37°C. The FITC-labeled TUNEL-positive cells were imaged by fluorescent microscopy at 488 nm excitation and 530 nm emission. Cells were quantified by counting 100 cells from 10 random microscopic fields.

### Western blot analysis

Cells for analysis were lysed in ice for 30 min after washing with pre-cooled PBS. The protein supernatants determined by the bicinchoninic acid (BCA) method were separated by

10% sodium dodecyl sulfate-polyacrylamide gel electrophoresis (SDS-PAGE) gels, then electrotransferred onto polyvinylidene difluoride (PVDF) membranes. After blocking with 5% fat-free dry milk in Tris-buffered saline with Tween 20 (TBST) buffer for 30 min, the membranes were immunoblotted with primary antibody solutions at 4°C overnight. After washing 3 times with TBST, HRP-conjugated secondary antibody solutions were applied for 1 h at 37°C. The Tanon 2500 Gel Imaging System (Shanghai, China) was used to detect the blots visualized by enhanced chemiluminescence (ECL) detection reagent (Millipore, Darmstadt, Germany). Protein band intensities were quantified by densitometric analysis using ImageJ software (National Institutes of Health, USA).

### Immunofluorescence staining

PC cells ( $1 \times 10^5$ ) were cultured in 12-well plates for 12 h, then exposed to irisin alone, DOX alone, or DOX in combination with irisin for 24 h. Cells were fixed with 4% paraformaldehyde for 20 min and permeabilized with 0.5% Triton X-100 for 15 min. Then, cells were blocked with 3% BSA for 1 h, and incubated with Anti-NF- $\kappa\text{B}$  p65 rabbit antibody at 37°C for 1 h. After washing with PBS, FITC-anti-rabbit IgG antibody solutions were added to the cells for 1 h. Cells were then counter-stained with Hoechst 33258 and observed under a fluorescence microscope.

### Statistical analysis

Data were analyzed statistically using the two-tailed unpaired *t* test for comparison of 2 groups or by one-way ANOVA (analysis of variance), followed by Tukey post hoc tests for comparison of more than 2 groups, with GraphPad Prism 5.0 software.  $P < 0.05$  was considered statistically significant. Data are presented as the mean  $\pm$  standard error of the mean (SEM).

## Results

### Irisin enhances the inhibitory effects of DOX in PC cells

To evaluate the cytotoxicity of DOX with or without irisin, MIA PaCa-2 and BxPC-3 cells were incubated with 7 concentrations of DOX ranging from 0.375 to 24  $\mu\text{g}/\text{mL}$  combined with various concentrations (5, 10, 50, 100 nM) of irisin for 24 h. The viabilities of MIA PaCa-2 (Figure 1Aa) and BxPC-3 (Figure 1Ab) cells were both inhibited by DOX compared to the control group. In addition, the inhibitory effects increased with increasing concentration of irisin. Results showed that in cells treated with DOX and 100 nM irisin, the  $\text{IC}_{50}$  value of DOX ( $0.805 \pm 0.037$   $\mu\text{g}/\text{mL}$ ) was significantly lower than that in MIA PaCa-2 cells treated with DOX alone ( $1.145 \pm 0.008$   $\mu\text{g}/\text{mL}$ ;  $P = 0.009$ ) (Figure 1Ba). Similar results were also observed in BxPC-3 cells (Figure 1Bb), and the  $\text{IC}_{50}$

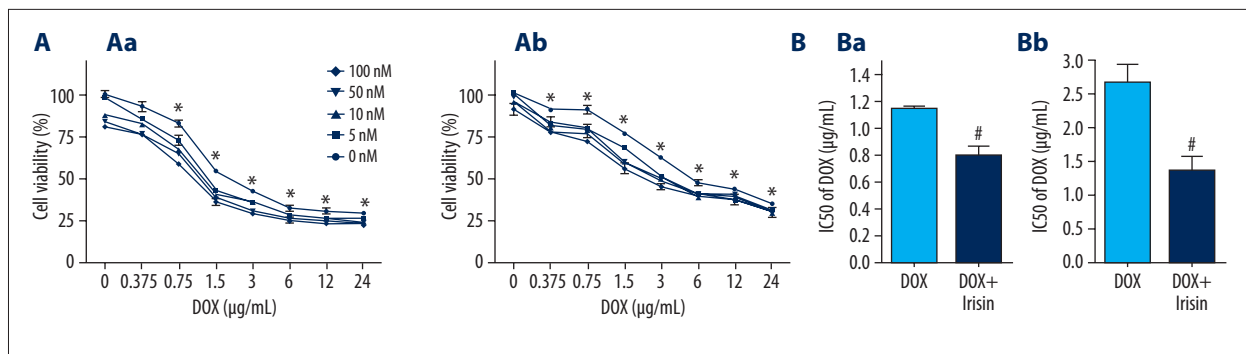


**Figure 1.** Irisin enhances the inhibitory effects of DOX in PC cells. (A) MIA PaCa-2 (a) and BxPC-3 (b) cells were treated with different concentrations of DOX (0, 0.375, 0.75, 1.5, 3, 6, 12, and 24  $\mu\text{g/mL}$ ) combined with different concentrations of irisin (0, 5, 10, 50, and 100 nM) for 24 h. Cell viabilities were then measured by MTT assay. (B)  $\text{IC}_{50}$  of DOX to MIA PaCa-2 (a) and BxPC-3 (b) cells. Error bars represent SEM. \*  $P<0.05$  compared with the control group. #  $P<0.05$  compared with the DOX-treated group.

value of DOX ( $1.349\pm 0.129 \mu\text{g/mL}$ ) in the combined group was significantly lower than that ( $2.682\pm 0.151 \mu\text{g/mL}$ ;  $P=0.002$ ) in the DOX-treated group. The 0.75  $\mu\text{g/mL}$  and 1.5  $\mu\text{g/mL}$  were chosen for the follow-up experiments as they were the nearest to the concentrations of DOX (0, 0.375, 0.75, 1.5, 3, 6, 12, and 24  $\mu\text{g/mL}$ ) to  $\text{IC}_{50}$  of DOX in the presence of 100 nM irisin. Therefore, the data indicated that irisin enhanced the chemosensitivity to DOX in PC cells.

#### Irisin enhances the chemosensitivity of PC cells to GEM

To evaluate the cytotoxicity of GEM with or without irisin, MIA PaCa-2 and BxPC-3 cells were incubated with 7 concentrations of GEM ranging from 0.375 to 48  $\mu\text{g/mL}$  combined with various concentrations (5, 10, 50, 100 nM) of irisin for 48 h. The viabilities of MIA PaCa-2 (Figure 2Aa) and BxPC-3 (Figure 2Ab) cells were inhibited by GEM compared to the control group. Moreover, results showed that the  $\text{IC}_{50}$  value of GEM ( $8.912\pm 0.221 \mu\text{g/mL}$ ) in the combined group was significantly lower than that in the GEM alone group ( $15.61\pm 0.636 \mu\text{g/mL}$ ;  $P=0.0006$ ) (Figure 2Ba) in MIA PaCa-2 cells. Similar results were also observed in BxPC-3 cells (Figure 2Bb), and the  $\text{IC}_{50}$  value of GEM ( $20.11\pm 1.019 \mu\text{g/mL}$ ) in the combined group was significantly lower than that of the GEM-treated group ( $27.35\pm 2.194 \mu\text{g/mL}$ ;  $P=0.043$ ). The concentrations of 9  $\mu\text{g/mL}$  and 15  $\mu\text{g/mL}$  were chosen for the apoptosis assay as they were near the  $\text{IC}_{50}$  concentrations of GEM in the presence of 100 nM irisin. Flow cytometry was used to detect cells apoptosis. The results shown in Figure 2C and 2D suggested that the percentage of apoptotic cells was higher in the GEM and irisin combined group in BxPC-3 cells (Figure 2Cb, 2Db). In contrast, the percentage of apoptotic cells was not increased in MIA PaCa-2 (Figure 2Ca, 2Da).

#### Irisin enhances DOX-induced apoptosis in PC cells

To explore the role of irisin in increasing DOX-induced inhibition of PC cell viabilities, cell apoptosis was assessed by TUNEL assay, and the expression of cleaved PARP, cleaved caspase-3, BCL-2, and BCL-xL were evaluated by Western blotting. As shown in Figure 3A and 3B, the numbers of TUNEL-positive apoptotic cells in the combined group in MIA PaCa-2 cells ( $20.40\pm 1.318\%$ ) and in BxPC-3 cells ( $14.60\pm 0.9333\%$ ) were significantly increased compared to the control group in MIA PaCa-2 cells (Figure 3Aa, 3Ba) ( $13.70\pm 0.8172\%$ ) and in BxPC-3 cells (Figure 3Ab, 3Bb) ( $9.900\pm 1.120\%$ ). After the enhancement effects of irisin on DOX-induced apoptosis were detected, the apoptosis-associated proteins were further investigated. The results showed that the expression levels of cleaved PARP and cleaved caspase-3 were both increased in the combination group compared to the DOX alone group (Figure 3C, 3D). In addition, there was notable downregulation of BCL-2 and BCL-xL expression in MIA PaCa-2 (Figure 3Ca, 3Da) and BxPC-3 (Figure 3Cb, 3Db) cells in the combined group. Collectively, these results demonstrated that irisin enhanced DOX-induced apoptosis, increased caspase-3 activity, and decreased the levels of anti-apoptotic proteins in PC cells.

#### Irisin decreases DOX accumulation in the PC cells

Fluorescence microscope and flow cytometry experiments were performed to assess the intracellular accumulation of DOX. As shown in Figure 4A, the spontaneous red fluorescence of DOX was weaker in the combined groups than in the DOX alone group. As shown in Figure 4B and 4C, lower fluorescence intensity was detected in the DOX co-treated with irisin groups compared to the DOX alone groups in MIA PaCa-2 (a) and Bxpc-3 (b) cells. Taken together, these results showed that irisin significantly decreased the intracellular accumulation of DOX in PC cells.



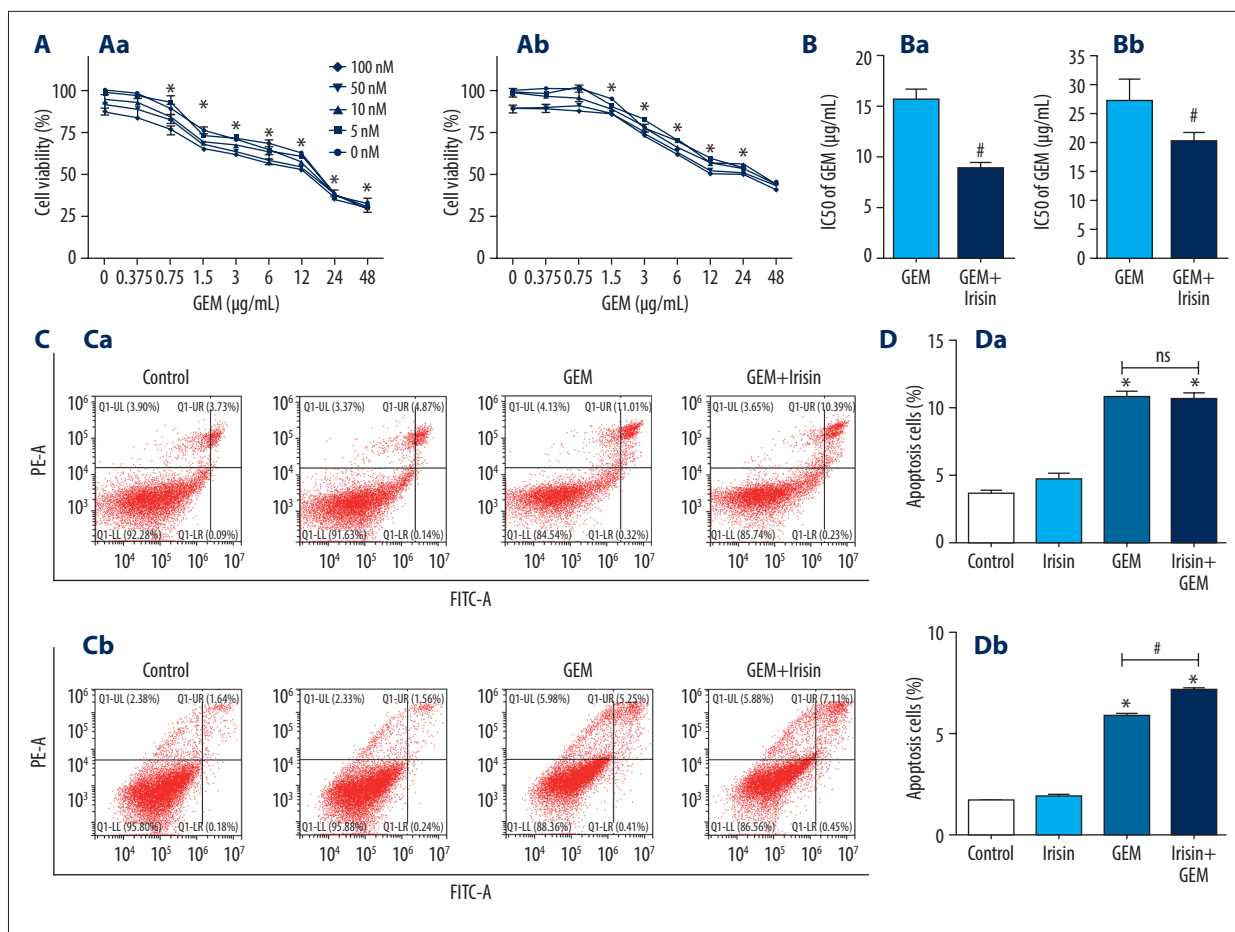


**Figure 2.** Irisin enhances the chemosensitivity of PC cells to gemcitabine. **(A)** MIA PaCa-2 **(a)** and BxPC-3 **(b)** cells were treated with different concentrations of GEM (0, 0.375, 0.75, 1.5, 3, 6, 12, 24, and 48 µg/mL) combined with different concentrations of irisin (0, 5, 10, 50, and 100 nM) for 48 h. Cell viabilities were then measured by MTT assay. **(B)** IC<sub>50</sub> of GEM to MIA PaCa-2 **(a)** and BxPC-3 **(b)** cells. Error bars represent SEM. \* *P*<0.05 compared with the control group. # *P*<0.05 compared with the GEM-treated group. **(C)** MIA PaCa-2 were exposed to 100 nM irisin alone, 9 µg/mL GEM alone, or GEM combined with irisin for 48 h. BxPC-3 cells were exposed to 100 nM irisin alone, 15 µg/mL GEM alone, or GEM combined with irisin for 48 h. The apoptotic rate in MIA PaCa-2 **(a)** and BxPC-3 **(b)** cells was analyzed using flow cytometry. **(D)** Quantification of apoptotic cells in MIA PaCa-2 **(a)** and BxPC-3 **(b)** cells. Error bars represent SEM. \* *P*<0.05 compared with the control group. # *P*<0.05 compared with the GEM-treated group.

### Irisin increases the chemosensitivity of PC cells to DOX via inhibition of the PI3K/AKT and NF-κB signaling pathways

In the present study, the effects of irisin and DOX on the expression of p-AKT in PC cells were assessed. Cells were analyzed at various treatment time points between 1 h and 24 h. Western blot analysis showed that the phosphorylation levels of AKT were decreased by irisin in a time-dependent manner (Supplementary Figure 1Aa, 1Ba), suggesting that irisin blocked the activations of the PI3K/AKT pathway in MIA PaCa-2 and BxPC-3 cells. The levels of p-AKT increased after brief (1 h) treatment with DOX and then decreased (Supplementary Figure 1Ab, 1Bb). As shown in Figure 5A and 5B, DOX alone, irisin alone, and their combination reduced the phosphorylation levels of AKT in MIA PaCa-2 (Figure 5Aa, 5Ba) and BxPC-3

(Figure 5Ab, 5Bb) cells after 24-h treatment, and the p-AKT change was significantly greater in the combined group. In addition, DOX significantly increased p-p65 and decreased the expression of IκB-α in MIA PaCa-2 (Figure 5Aa, 5Ba) and BxPC-3 cells (Figure 5Ab, 5Bb). However, irisin significantly suppressed phosphorylation of p65 and prevented the decline in IκB-α. As shown in Figure 5C, after exposure to DOX, NF-κB p65 translocations were observed in the nuclei in MIA PaCa-2 **(a)** and BxPC-3 **(b)** cells; however, DOX-induced translocations of p65 to nucleus were suppressed in the irisin and DOX combined group. Hence, the results suggested that inhibition of the AKT pathway and suppression of the NF-κB pathway play a critical role in the mechanism of irisin-enhanced chemosensitivity of PC cells to DOX.

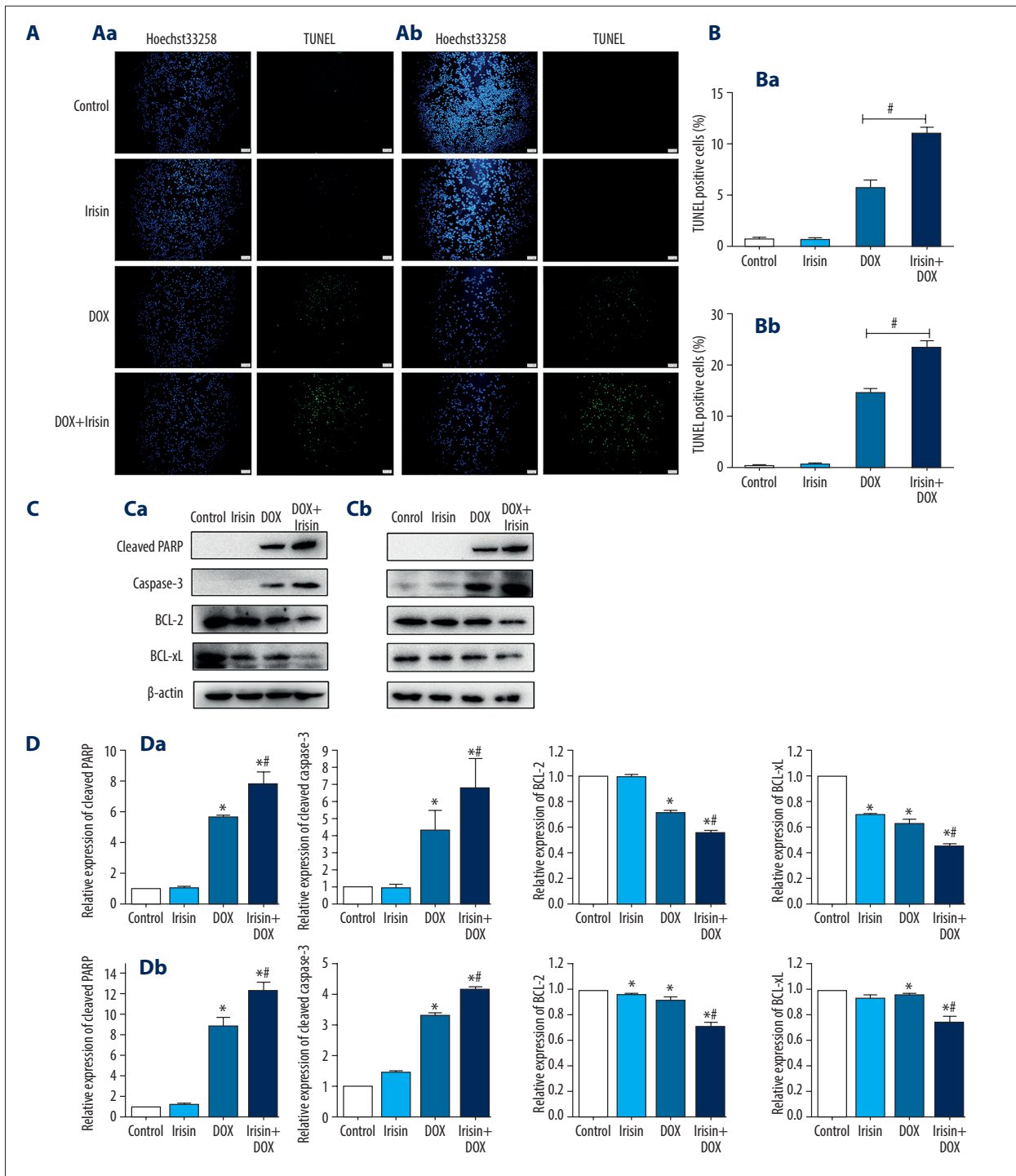


**Figure 3.** Irisin enhances DOX-induced apoptosis in PC cells. MIA PaCa-2 cells were exposed to 100 nM irisin alone, 0.75 µg/mL DOX alone, or DOX combined with irisin for 24 h. BxPC-3 cells were exposed to 100 nM irisin alone, 1.5 µg/mL DOX alone, or DOX combined with irisin for 24 h. (A) Images (40×) of TUNEL-positive MIA PaCa-2 (a) and BxPC-3 (b) cells are shown; apoptotic nuclei were identified by TUNEL staining (green), and total nuclei were identified by Hoechst 33258 counterstaining (blue). Scale bars: 200 µm. (B) Quantification of apoptotic-positive cells in MIA PaCa-2 (a) and BxPC-3 (b) cells. Error bars represent SEM. # *P*<0.05 compared with the DOX-treated group. (C) Western blot analysis of the levels of cleaved PARP, cleaved caspase-3, BCL-2, and BCL-xL protein in MIA PaCa-2 (a) and BxPC-3 (b) cells. β-actin served as the loading control. (D) Quantitation of protein expression in MIA PaCa-2 (a) and BxPC-3 (b) cells. Error bars represent SEM. \* *P*<0.05 compared with the control group. # *P*<0.05 compared with the DOX-treated group.

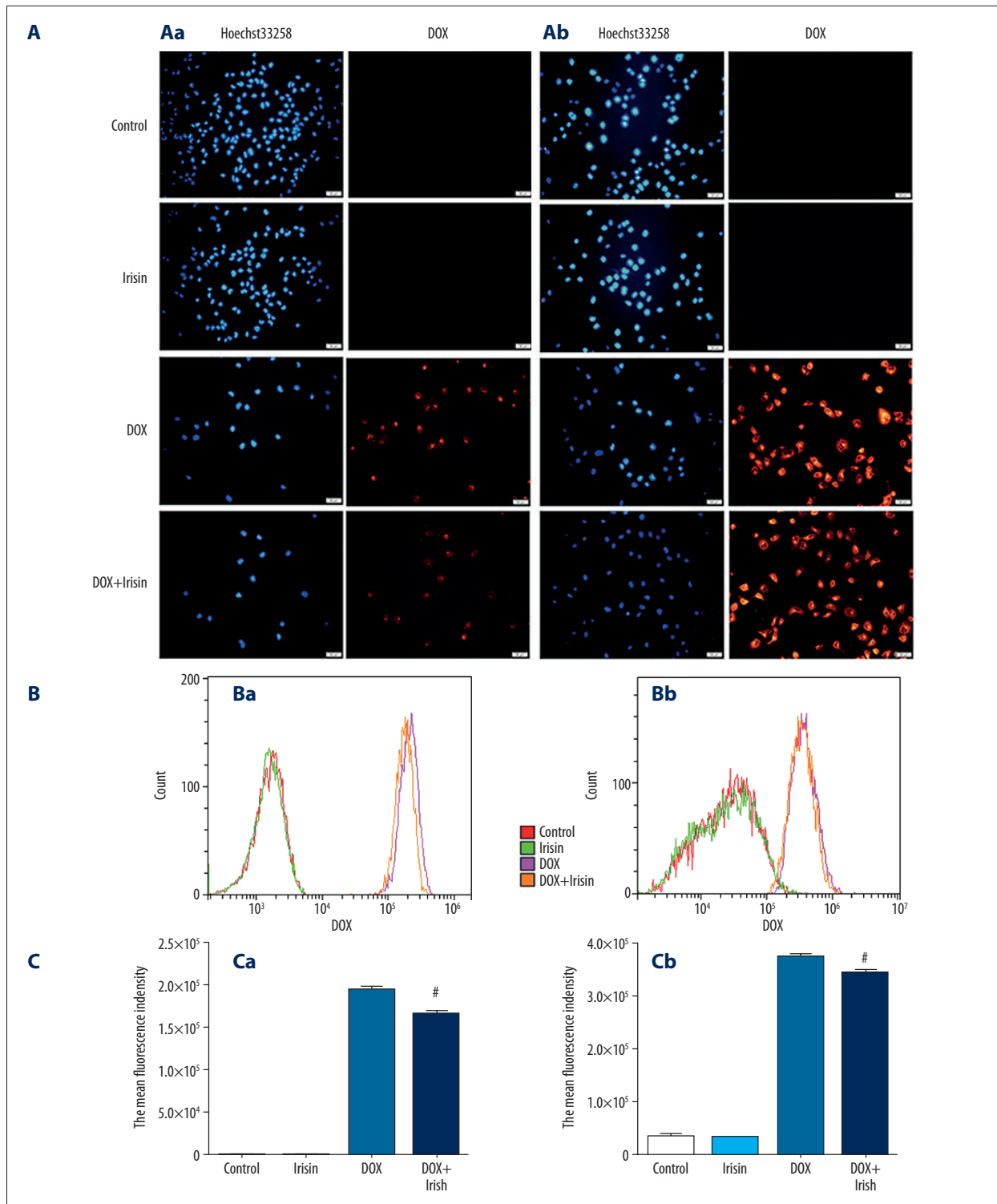


**Figure 4.** Irisin decreased DOX accumulation in the PC cells. MIA PaCa-2 were exposed to 100 nM irisin alone, 0.75 µg/mL DOX alone, or DOX combined with irisin for 24 h. Bxpc-3 cells were exposed to 100 nM irisin alone, 1.5 µg/mL DOX alone, or DOX combined with irisin for 24 h. (A) Fluorescence microscopy images (200×) showing DOX accumulation in MIA PaCa-2 (a) and Bxpc-3 (b) cells, DOX: red, hoechst33258: blue. Scale bars: 50 µm. (B) The cells were collected for measurement of DOX fluorescence in MIA PaCa-2 (a) and Bxpc-3 (b) cells using flow cytometry. (C) Quantitative comparison of fluorescence intensity in MIA PaCa-2 (a) and Bxpc-3 (b) cells. #  $P < 0.05$  compared with the DOX-treated group.

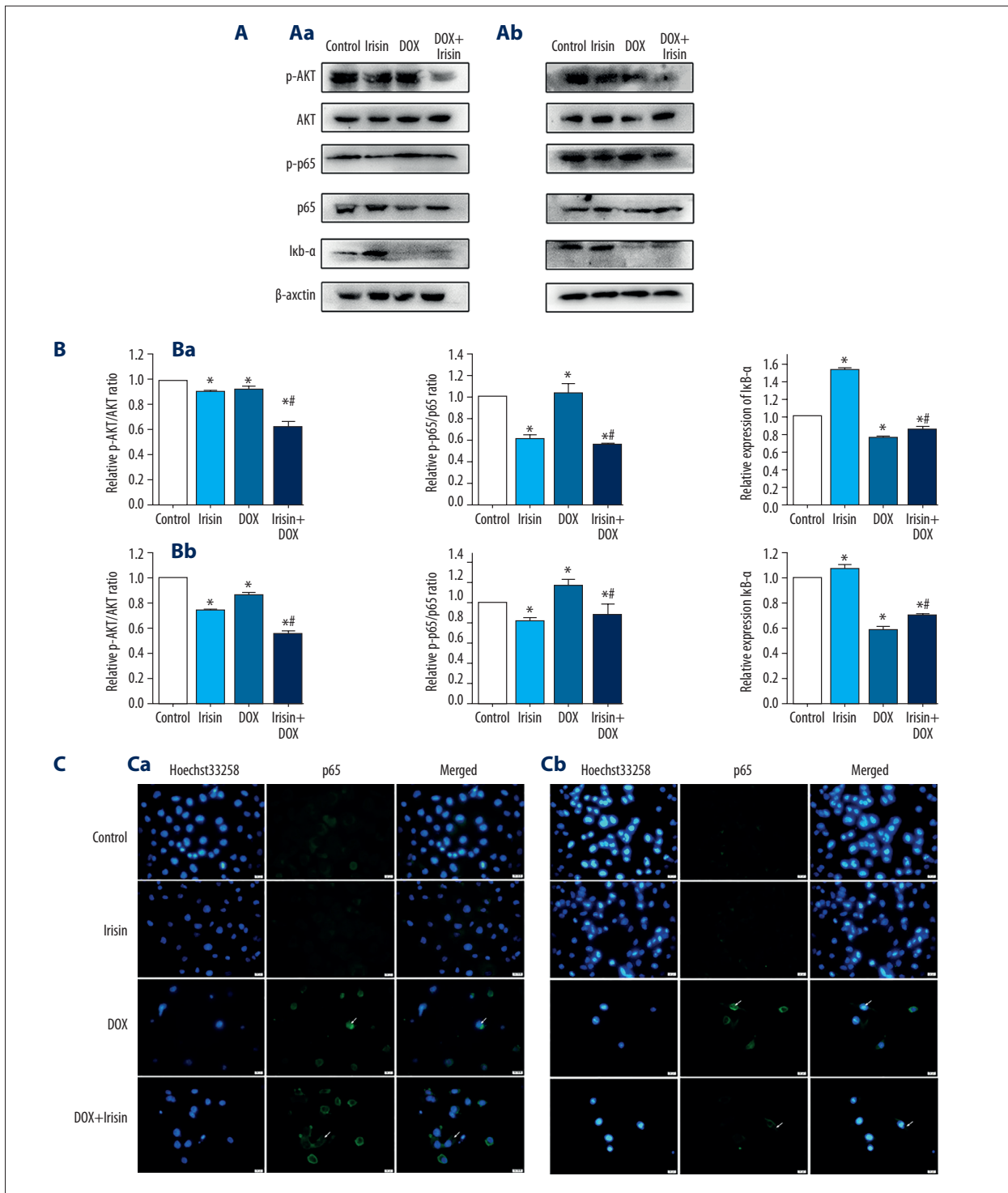


**Figure 5.** Irisin increased the chemosensitivity of PC cells to DOX via inhibition of the PI3K/AKT and NF-κB signaling pathways. MIA PaCa-2 cells were exposed to 100 nM irisin alone, 0.75 μg/mL DOX alone, or DOX combined with irisin for 24 h. BxPC-3 cells were exposed to 100 nM irisin alone, 1.5 μg/mL DOX alone, or DOX combined with irisin for 24 h. **(A)** Western blot analysis of p-AKT, AKT, p-p65 (p-NF-κB), p65 (NF-κB), and IκB-α in MIA PaCa-2 **(a)** and BxPC-3 **(b)** cells. β-actin served as the loading control. **(B)** Quantitation of protein expression in MIA PaCa-2 **(a)** and BxPC-3 **(b)** cells. Error bars represent SEM. \*  $P < 0.05$  compared with the control group. #  $P < 0.05$  compared with the DOX-treated group. **(C)** Images (400×) of the accumulation of p65 in nucleus in MIA paca-2 **(a)** and BxPC-3 **(b)** cells. p65: Green; Hoechst 33258: Blue. Scale bars: 20 μm.



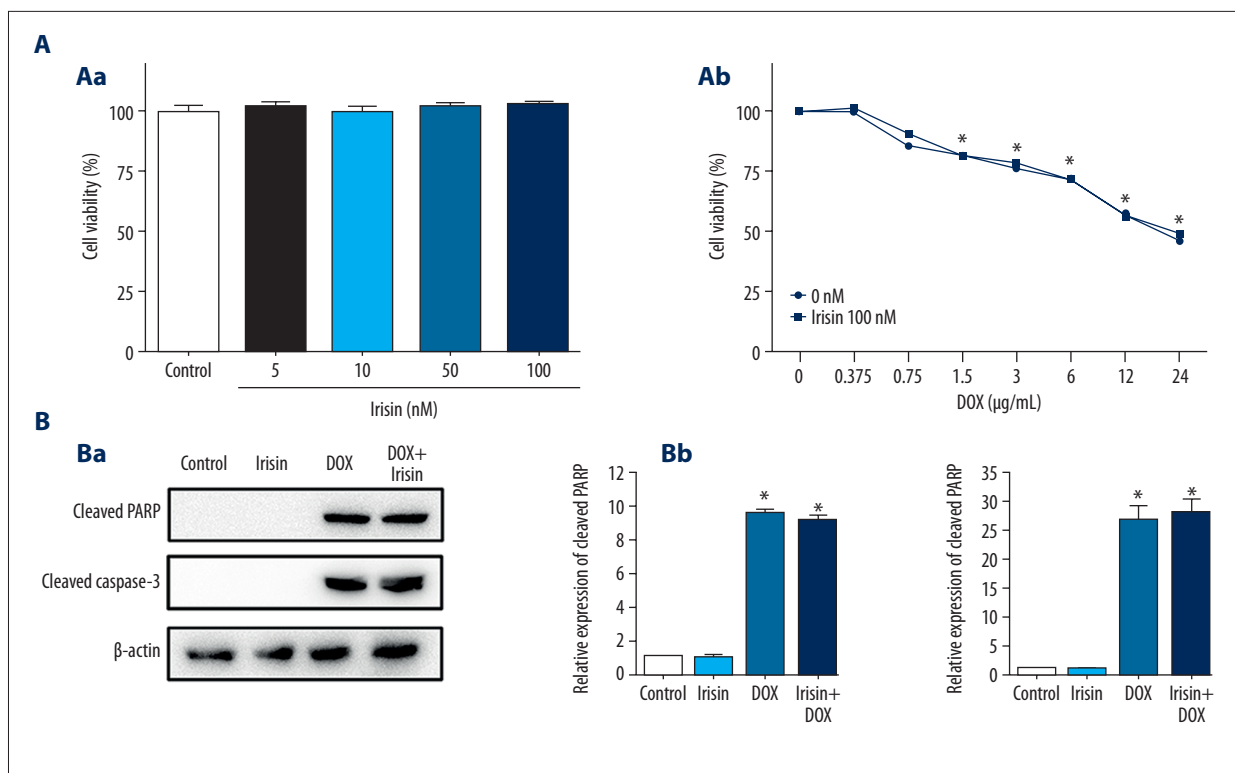


**Figure 6.** Irisin had no effects on DOX-induced cardiotoxicity. **(A)** (a) H9c2 cells were treated with different concentrations of irisin (0, 5, 10, 50, and 100 nM). (b) H9c2 cells were treated with different concentrations of DOX (0, 0.375, 0.75, 1.5, 3, 6, 12, and 24 µg/mL) combined with 100 nM irisin. Cell viabilities were measured by MTT assay. **(B)** H9c2 cells were exposed to 100 nM irisin alone, 3 µg/mL DOX alone, or DOX combined with irisin for 24 h. **(a)** Western blot analysis of cleaved PARP and cleaved caspase-3 in H9c2 cells. β-actin served as the loading control. **(b)** Quantitation of protein expression in H9c2 cells. Error bars represent SEM. \*  $P < 0.05$  compared with the control group.

### Irisin has no effects on DOX-induced cardiotoxicity

The effects of irisin on DOX-induced cardiotoxicity were studied. Irisin had no effect on the viabilities of H9c2 cells after 24-h treatment (Figure 6Aa), while DOX significantly impaired the viabilities in H9c2 cells after 24-h treatment (Figure 6Ab). Moreover, the expression levels of cleaved PARP and cleaved caspase-3 were markedly increased in H9c2 cells (Figure 6Ba, 6Bb). However, there were no protective or aggravating effects of irisin (Figure 6Ab) on DOX-induced injury to myocardial cells. The apoptotic rate of H9c2 cells and expression levels of cleaved PARP and cleaved caspase3 were not increased in the combination group compared to the DOX alone group (Figure 6Ba, 6Bb). Therefore, the results demonstrated that irisin has no effects on the cardiotoxicity caused by DOX during 24-h treatment.

### Discussion

PC is currently one of the deadliest solid malignancies, and surgery is the preferred treatment for patients in the early

stages of the disease. Patients with stage III locally advanced disease should be treated with chemotherapy and/or chemoradiotherapy [1], but more effective therapeutic options for PC are required. Studies showed that patients with type 2 diabetes have a 1.8-fold increased risk of PC compared with non-diabetics [22]. Irisin has been reported to influence various metabolic diseases [18,32–34]. Significantly lower levels of irisin were observed in patients with type 2 diabetes mellitus compared with non-diabetic individuals [32,33]. Recent studies showed that irisin can inhibit the development of cancer cells, including breast cancer [24], osteosarcoma [35], lung cancer [25], and PC [31]. In addition, it has been reported that irisin can enhance the cytotoxic effects of DOX on malignant breast epithelial cells through inhibiting NF-κB activation [24]. Serum irisin levels were increased in DOX-treated rats, which indicates a role for irisin in DOX treatment of tumors [36]. In the present study, PC cells were processed with irisin combined with DOX or GEM. Combined treatment with irisin and DOX or GEM resulted in a remarkable decrease of the  $IC_{50}$  of the chemotherapeutic drugs DOX and GEM. However, slight effects of GEM on inducing apoptosis were observed in MIA PaCa-2 cells but not in BxPC-3 cells. Irisin combined with DOX

significantly increased apoptosis in MIA PaCa-2 and BxPC-3 cells as identified by TUNEL assay. These results suggest that irisin has different effects on different chemotherapy drugs, which may be due to the mechanism of action of the chemotherapy drugs and irisin [35,37,38]. It has been reported that DOX can induce intrinsic apoptosis in PC cells through regulating BCL-2 and caspase proteins [28,39]. Cleaved caspase-3 marks the end of the downstream effect of the caspases and irreversibly destroys PARP protein during apoptosis, while BCL-2 is vital for mitochondria-mediated apoptosis [39]. Therefore, cleaved caspase-3, cleaved PARP, and pro-apoptotic proteins (BCL-2, BCL-xL) were investigated in this study. It was interesting to find that irisin combined with DOX caused increased levels of cleaved caspase-3 and cleaved PARP, while exacerbating the inhibition of BCL-2 and BCL-xL compared with DOX alone in PC cells. The results showed that irisin can sensitize PC cells to DOX treatment with decreasing DOX accumulation after 24-h treatment, which is consistent with the effect of irisin on the intracellular accumulation of DOX in breast cancer [24]. Lower uptake of DOX had more inhibition effect against MIA PaCa-2 and Bxpc-3 cells with the presence of irisin in this study, which suggested that irisin makes DOX more efficient against PC cells. The results indicated that irisin enhances apoptosis of PC cells through the mitochondrial signaling pathway. Many cancers, including PC, breast cancer, lung cancer, gastric cancer, and uterine cancer, have acquired resistance to DOX due to the enhanced survival signal of the PI3K pathway [28]. Previous reports have suggested that inhibition of the PI3K/AKT pathway is a possible mechanism for improving the sensitivity of tumors to drugs [40,41]. NF- $\kappa$ B is an important downstream element of AKT [11]. High nuclear NF- $\kappa$ B p65 expression has been reported have associations with poor response to chemotherapy in cancer cell lines [9,11]. In tilapia pituitary cells, irisin inhibited growth hormone gene expression and secretion by inhibiting PI3K/AKT [42]. Another study demonstrated that irisin inhibited epithelial-mesenchymal-transition (EMT) and reduced the invasion of lung cancer cells via mediating the PI3K/AKT/Snail signaling pathway [25]. In addition, irisin has been found to suppress NF- $\kappa$ B activation [24]. To elucidate the mechanisms involved in irisin-enhancement of DOX-induced apoptosis, PI3K/AKT/NF- $\kappa$ B signaling was examined in this study. The results suggested that irisin inhibited AKT signaling in PC cells in a time-dependent manner, which was

consistent with previously published studies, and the results were confirmed. After treatment with irisin or DOX for 24 h, the expression levels of p-AKT were downregulated in both 2 PC cell lines in this study. Moreover, irisin enhanced the suppression of p-AKT and inhibited the activation of NF- $\kappa$ B signaling when used in combination with DOX. In recent years, the combinations of therapeutic molecules and chemotherapy drugs have been reported and provide a novel insight into PC treatment [43–45]. The results revealed that irisin sensitized PC cells to DOX and GEM, and represents a novel therapeutic molecule to prevent PC. Considering DOX-induced cardiotoxicity, we investigated whether irisin has a role in DOX-induced H9c2 myocardial cell injury. Our results demonstrated that irisin neither ameliorated nor aggravated DOX-induced toxicity in H9c2 cells after 24-h treatment. The highest concentration of exogenous irisin used in this study was 100 nM, and it has been reported that 50 nM and 100 nM are the pharmacological concentrations of irisin [46]. At certain concentrations, irisin can increase myocardial cell metabolism, inhibit cell proliferation, and promote cell differentiation at 72 h in H9c2 cells by activating the PI3K/AKT pathway [47]. Thus, it seems that longer treatment time with irisin in H9c2 cells, and *in vivo* studies may be needed to further explore its effects on DOX-induced myocardial cell injury.

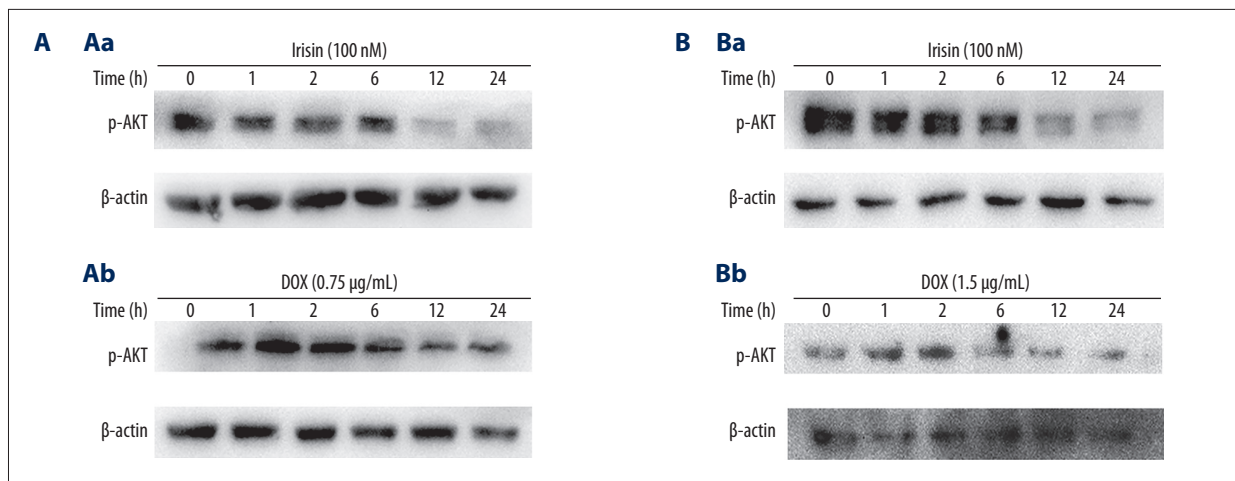
## Conclusions

We showed that irisin can increase the chemosensitivity of PC cells to DOX or GEM and enhance DOX-induced apoptosis in PC cancer cells through upregulating cleaved PARP and cleaved caspase-3 and downregulating Bcl-2, BCL-xL, and PI3K/AKT/NF- $\kappa$ B signaling pathway. These results show that combination treatment with DOX and irisin can decrease the dose of DOX but provide similar therapeutic results in clinical practice. Hence, irisin could be used as an adjunctive agent combined with chemotherapy and provides a new approach for the treatment of PC cells.

## Conflict of interest

None.

## Supplementary Figure



**Supplementary Figure 1.** Western blot analysis of p-AKT in PC cells. (A) Western blot analysis of p-AKT in treated MIA PaCa-2 cells obtained at different time points for irisin (a) and DOX (b) treatment with β-actin as the loading control. (B) Western blot analysis of p-AKT in treated BxPC-3 cells obtained at different time points for irisin (a) and DOX (b) treatment with β-actin as the loading control.

## References:

- Tan CR, Yaffee PM, Jamil LH et al: Pancreatic cancer cachexia: A review of mechanisms and therapeutics. *Front Physiol*, 2014; 5: 88
- Wolfgang CL, Herman JM, Laheru DA et al: Recent progress in pancreatic cancer. *Cancer J Clin*, 2013; 63: 318–48
- Siegel RL, Miller KD, Jemal A: Cancer statistics, 2016. *Cancer J Clin*, 2016; 66: 7–30
- Yang SH, Shao YY, Lin CC et al: A phase I study of S-1-based concurrent chemoradiotherapy followed by gemcitabine and S-1 in metastatic pancreatic adenocarcinoma. *Anticancer Res*, 2018; 38: 4805–12
- Yang F, Teves SS, Kemp CJ, Henikoff S: Doxorubicin, DNA torsion, and chromatin dynamics. *Biochim Biophys Acta*, 2014; 1845: 84–89
- Ni S, Qiu L, Zhang G, Zhou H, Han Y: Lymph cancer chemotherapy: Delivery of doxorubicin-gemcitabine prodrug and vincristine by nanostructured lipid carriers. *Int J Nanomedicine*, 2017; 12: 1565–76
- Xiong XB, Lavasanifar A: Traceable multifunctional micellar nanocarriers for cancer-targeted co-delivery of MDR-1 siRNA and doxorubicin. *ACS Nano*, 2011; 5: 5202–13
- Li K, Liu W, Zhao Q et al: Combination of tanshinone IIA and doxorubicin possesses synergism and attenuation effects on doxorubicin in the treatment of breast cancer. *Phytother Res*, 2019; 33: 1658–69
- Eisa NH, ElSherbiny NM, Shebl AM et al: Phenethyl isothiocyanate potentiates anti-tumour effect of doxorubicin through Akt-dependent pathway. *Cell Biochem Funct*, 2015; 33: 541–51
- Geng X, Xie L, Xing H: PI3K inhibitor combined with chemotherapy can enhance the apoptosis of neuroblastoma cells *in vitro* and *in vivo*. *Technol Cancer Res Treat*, 2016; 15: 716–22
- Deeb D, Gao X, Liu YB et al: Pristimerin, a quinomethide triterpenoid, induces apoptosis in pancreatic cancer cells through the inhibition of pro-survival Akt/NF-kappaB/mTOR signaling proteins and anti-apoptotic Bcl-2. *Int J Oncol*, 2014; 44: 1707–15
- Xia J, Rong L, Sawakami T et al: Shufeng Jiedu Capsule and its active ingredients induce apoptosis, inhibit migration and invasion, and enhances doxorubicin therapeutic efficacy in hepatocellular carcinoma. *Biomed Pharmacother*, 2018; 99: 921–30
- Zou W, Ma X, Hua W et al: Caveolin-1 mediates chemoresistance in cisplatin-resistant ovarian cancer cells by targeting apoptosis through the Notch-1/Akt/NF-kappaB pathway. *Oncol Rep*, 2015; 34: 3256–63
- Mon MT, Yodkeeree S, Punfa W et al: Alkaloids from *Stephania venosa* as chemo-sensitizers in SKOV3 ovarian cancer cells via Akt/NF-kappaB signaling. *Chem Pharm Bull (Tokyo)*, 2018; 66: 162–69
- Maier HJ, Schmidt-Strassburger U, Huber MA et al: NF-kappaB promotes epithelial-mesenchymal transition, migration and invasion of pancreatic carcinoma cells. *Cancer Lett*, 2010; 295: 214–28
- Cheng H, Lu C, Tang R et al: Ellagic acid inhibits the proliferation of human pancreatic carcinoma PANC-1 cells *in vitro* and *in vivo*. *Oncotarget*, 2017; 8: 12301–10
- Bostrom P, Wu J, Jedrychowski MP et al: A PGC1-alpha-dependent myokine that drives brown-fat-like development of white fat and thermogenesis. *Nature*, 2012; 481: 463–68
- Arias-Loste MT, Ranchal I, Romero-Gomez M, Crespo J: Irisin, a link among fatty liver disease, physical inactivity and insulin resistance. *Int J Mol Sci*, 2014; 15: 23163–78
- Bastu E, Zeybek U, Gurevin EG et al: Effects of irisin and exercise on metabolic parameters and reproductive hormone levels in high-fat diet-induced obese female mice. *Reprod Sci*, 2018; 25: 281–91
- Leung PS: The potential of irisin as a therapeutic for diabetes. *Future Med Chem*, 2017; 9: 529–32
- Wang H, Zhang SY, Zhao YT et al: Abstract 17950: Irisin protects the heart against myocardial ischemia and reperfusion injury. *Circulation*, 2016; 134: A17950
- Pothuraju R, Rachagani S, Junker WM et al: Pancreatic cancer associated with obesity and diabetes: An alternative approach for its targeting. *J Exp Clin Cancer Res*, 2018; 37: 319
- Aydin S, Kuloglu T, Ozercan MR et al: Irisin immunohistochemistry in gastrointestinal system cancers. *Biotech Histochem*, 2016; 91: 242–50
- Gannon NP, Vaughan RA, Garcia-Smith R et al: Effects of the exercise-inducible myokine irisin on malignant and non-malignant breast epithelial cell behavior *in vitro*. *Int J Cancer*, 2015; 136: E197–202
- Shao L, Li H, Chen J et al: Irisin suppresses the migration, proliferation, and invasion of lung cancer cells via inhibition of epithelial-to-mesenchymal transition. *Biochem Biophys Res Commun*, 2017; 485: 598–605
- Han F, Zhang S, Hou N et al: Irisin improves endothelial function in obese mice through the AMPK-eNOS pathway. *Am J Physiol Heart Circ Physiol*, 2015; 309: H1501–8

27. Shi G, Tang N, Qiu J et al: Irisin stimulates cell proliferation and invasion by targeting the PI3K/AKT pathway in human hepatocellular carcinoma. *Biochem Biophys Res Commun*, 2017; 493: 585–91
28. Durrant DE, Das A, Dyer S et al: targeted inhibition of phosphoinositide 3-kinase/mammalian target of rapamycin sensitizes pancreatic cancer cells to doxorubicin without exacerbating cardiac toxicity. *Mol Pharmacol*, 2015; 88: 512–23
29. Bernard Y, Ribeiro N, Thuaud F et al: Flavaglines alleviate doxorubicin cardiotoxicity: Implication of Hsp27. *PLoS One*, 2011; 6: e25302
30. Zhou Q, Zhou Y, Liu X, Shen Y: GDC-0449 improves the antitumor activity of nano-doxorubicin in pancreatic cancer in a fibroblast-enriched microenvironment. *Sci Rep*, 2017; 7: 13379
31. Liu J, Song N, Huang Y, Chen Y: Irisin inhibits pancreatic cancer cell growth via the AMPK-mTOR pathway. *Sci Rep*, 2018; 8: 15247
32. Moreno-Navarrete JM, Ortega F, Serrano M et al: Irisin is expressed and produced by human muscle and adipose tissue in association with obesity and insulin resistance. *J Clin Endocrinol Metab*, 2013; 98: E769–78
33. Duan H, Ma B, Ma X et al: Anti-diabetic activity of recombinant irisin in STZ-induced insulin-deficient diabetic mice. *Int J Biol Macromol*, 2016; 84: 457–63
34. Gizaw M, Anandakumar P, Debela T: A review on the role of irisin in insulin resistance and type 2 diabetes mellitus. *J Pharmacopuncture*, 2017; 20: 235–42
35. Kong G, Jiang Y, Sun X et al: Irisin reverses the IL-6 induced epithelial-mesenchymal transition in osteosarcoma cell migration and invasion through the STAT3/Snail signaling pathway. *Oncol Rep*, 2017; 38: 2647–56
36. Aydin S, Eren MN, Kuloglu T et al: Alteration of serum and cardiac tissue adropin, copeptin, irisin and TRPM2 expressions in DOX treated male rats. *Biotech Histochem*, 2015; 90: 197–205
37. Li RL, Wu SS, Wu Y et al: Irisin alleviates pressure overload-induced cardiac hypertrophy by inducing protective autophagy via mTOR-independent activation of the AMPK-ULK1 pathway. *J Mol Cell Cardiol*, 2018; 121: 242–55
38. Song H, Wu F, Zhang Y et al: Irisin promotes human umbilical vein endothelial cell proliferation through the ERK signaling pathway and partly suppresses high glucose-induced apoptosis. *PLoS One*, 2014; 9: e110273
39. Van Opdenbosch N, Lamkanfi M: Caspases in cell death, inflammation, and disease. *Immunity*, 2019; 50: 1352–64
40. Bender A, Opel D, Naumann I et al: PI3K inhibitors prime neuroblastoma cells for chemotherapy by shifting the balance towards pro-apoptotic Bcl-2 proteins and enhanced mitochondrial apoptosis. *Oncogene*, 2011; 30: 494–503
41. Ni F, Huang X, Chen Z et al: Shikonin exerts antitumor activity in Burkitt's lymphoma by inhibiting C-MYC and PI3K/AKT/mTOR pathway and acts synergistically with doxorubicin. *Sci Rep*, 2018; 8: 3317
42. Lian A, Li X, Jiang Q: Irisin inhibition of growth hormone secretion in cultured tilapia pituitary cells. *Mol Cell Endocrinol*, 2017; 439: 395–406
43. Zheng S, Wang X, Weng YH et al: siRNA knockdown of RRM2 effectively suppressed pancreatic tumor growth alone or synergistically with doxorubicin. *Mol Ther Nucleic Acids*, 2018; 12: 805–16
44. Zhao X, Wang X, Sun W et al: Precision design of nanomedicines to restore gemcitabine chemosensitivity for personalized pancreatic ductal adenocarcinoma treatment. *Biomaterials*, 2018; 158: 44–55
45. Ma T, Chen W, Zhi X et al: USP9X inhibition improves gemcitabine sensitivity in pancreatic cancer by inhibiting autophagy. *Cancer Lett*, 2018; 436: 129–38
46. Moon HS, Dincer F, Mantzoros CS: Pharmacological concentrations of irisin increase cell proliferation without influencing markers of neurite outgrowth and synaptogenesis in mouse H19-7 hippocampal cell lines. *Metabolism*, 2013; 62: 1131–36
47. Xie C, Zhang Y, Tran TD et al: Irisin controls growth, intracellular Ca<sup>2+</sup> signals, and mitochondrial thermogenesis in cardiomyoblasts. *PLoS One*, 2015; 10: e0136816